

**Magnetic shape memory effect in the paramagnetic state in  $RCu_2$  ( $R$ =rare earth) antiferromagnets**

Sebastian Raasch,\* Mathias Doerr, Andreas Kreyssig, and Michael Loewenhaupt  
*Institut für Festkörperphysik (IFP), Technische Universität Dresden, Dresden, Germany*

Martin Rotter  
*Institut für Physikalische Chemie, Universität Wien, Wien, Austria*

Jens-Uwe Hoffmann  
*Hahn-Meitner-Institut Berlin, Berlin, Germany*  
 (Received 11 August 2005; published 1 February 2006)

$RCu_2$  ( $R$ =rare earth) is presented as the first magnetic shape memory (MSM) alloy with the magnetic anisotropy of rare earth ions as impelling force. Besides  $La_{2-x}Sr_xCuO_4$   $RCu_2$  is the second known antiferromagnetic MSM-compound system. However, longrange magnetic order is not necessary for the MSM effect here. Microstructural changes are occurring even above the magnetic ordering temperature because the magnetic anisotropy gives a strong effect also in the paramagnetic state.  $RCu_2$  compounds have a pseudo-hexagonal orthorhombic structure which splits up into three twin variants, each rotated about  $60^\circ$  to the others about the *pseudo-hexagonal* axis. To move the twin boundaries, a magnetic field of about 3.2 T and a temperature of typical 30 K is necessary. Moving of twin boundaries results in a typical length change of two percent. Depending on the field direction a certain twin variant is favored. Neutron data from a  $Tb_{0.5}Dy_{0.5}Cu_2$  single crystal confirm a change of the volume fraction of the three twin variants.

DOI: [10.1103/PhysRevB.73.064402](https://doi.org/10.1103/PhysRevB.73.064402)

PACS number(s): 75.80.+q, 07.10.Cm, 81.16.Ta, 85.85.+j

**I. INTRODUCTION**

In 1990 Hashimoto *et al.* found a very huge jump in magnetization on  $DyCu_2$  by applying a high magnetic field along the magnetic hard  $c$  axis.<sup>1</sup> This observation has been the first indication of a magnetically induced conversionlike behavior which could also be found later in most of the other antiferromagnetic  $RCu_2$  compounds.<sup>2-7</sup> After the discovery many investigations of macroscopic properties like magnetization and strain measurements have been done. In 1994 Hashimoto achieved the first back conversion into the virgin state by reapplying the field along the original magnetic easy  $a$  axis.<sup>8</sup> As the magnetization properties of the hard and easy axis seem to exchange during the conversion, the observed effect had been called *Ising axis conversion effect*. It has been interpreted by Yoshida *et al.*<sup>9</sup> as a phase transition into a metamagnetic metastable state due to a switch of the quadrupole moment. Further magnetization experiments have shown very similar magnetic behavior for  $PrCu_2$ ,  $CeCu_2$ ,  $TbCu_2$ ,  $NdCu_2$ , and  $TmCu_2$ .<sup>2-7</sup> Macroscopically, the conversion is connected to a giant strain of about two percent first seen at  $PrCu_2$  by Takeuchi.<sup>10</sup> These models, however, do not consider a structural or microstructural change. One exception is a study by P. Svoboda *et al.* who observed already the structural change during the conversion by neutrons.<sup>11</sup> He had concluded the crystal converting into a stable hexagonal structure.

Here, a different explanation for the effects described above is presented—the *twin-variant model (TV model)*. The model is based on the concept of the magnetic shape memory effect<sup>12-14</sup> and will be described in detail in the first part of the paper. In the second part we will state a verification of the model by several experiments on  $Tb_{0.5}Dy_{0.5}Cu_2$ . Microstructural changes assumed by the model could be con-

firmed by neutron scattering experiments. Further we will present magnetization measurements and the dependence of the conversion field on temperature.

**II. THE TWIN-VARIANT MODEL**

A necessary condition for the MSM effect is the existence of a strong magnetocrystalline anisotropy which is provided in  $RCu_2$  by the single-ion anisotropy of the rare earth ions. A further condition is a martensitic state of different twin variants which are close to a higher symmetry. The magnetic anisotropy has to be strongly coupled to the lattice to move twin boundaries by the application of an external field.<sup>15,16</sup>

$RCu_2$  crystallizes in the orthorhombic  $CeCu_2$  type structure (*Imma*) which is close to a high symmetry hexagonal structure. In  $RCu_2$  the  $ac$  plane is a pseudo-hexagonal basal plane. The  $c/a$  ratio is close to  $\sqrt{3}=1.732$  for the ideal hexagonal structure in orthorhombic description used throughout the paper ( $c/a=1.697$  for  $R=Tb_{0.5}Dy_{0.5}$ ,  $T=55$  K,  $a=4.328$  Å,  $b=6.816$  Å,  $c=7.344$  Å). An additional deviation from an ideal hexagonal structure is the position of the rare earth atoms varying in  $c$  direction within the  $bc$  plane depicted in Fig. 1. The proximity of  $RCu_2$  to the hexagonal structure finally favors the occurrence of three twin variants.

One cannot rule out a transition from the low-symmetric (orthorhombic) low-temperature martensitic phase into a highly symmetric (hexagonal) high-temperature austenitic phase close to the melting point. However, until now, no report of such an hexagonal phase in  $RCu_2$  exists to our knowledge. Nevertheless, the three appearing orthorhombic twin variants in  $RCu_2$  fulfill the description of a martensitic state in the context of MSM.

An applied field with a major component within the pseudo-hexagonal  $ac$  plane considerably far away from the

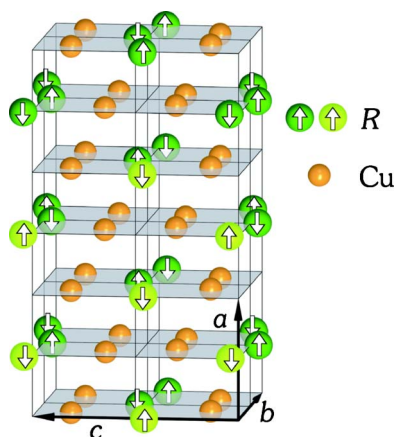


FIG. 1. (Color online) The crystallographic structure of  $RCu_2$ . The  $R$  atoms are alternately shifted in the  $c$  direction (true to scale). The arrows symbolize the antiferromagnetic structure for the case of  $R=Tb, Dy$ .

easy  $a$  axis effects an intrinsic strain due to magneto-elastic coupling. For a sufficient field  $H \parallel c$  we expect the crystal converting from a *one-variant state* into a *two-variant state* (compare Fig. 2), where the virgin variant is expected to vanish. The growth of new variants on cost of the virgin variant is usually described by the movement of a twin boundary connecting both variants. For  $Tb_{0.5}Dy_{0.5}Cu_2$  the new variants are *crystallographically* rotated by  $\alpha = \arctan(c/a) = \pm 60.52^\circ$  about the pseudohexagonal  $b$  axis (Fig. 2).

In practice, the crystal often broke into many pieces when the field had been applied. Geometrical considerations reveal an appropriate explanation for this difficulty. Due to the distortion  $c/a \neq \sqrt{3}$ , all three TVs cannot exist in the same crystal bordering each other without high mechanical stress. The stress origins from the geometrical misfit, for instance, at  $Tb_{0.5}Dy_{0.5}Cu_2$  a shearing of  $1.56^\circ$  ( $3 \times 60.52^\circ - 180^\circ$

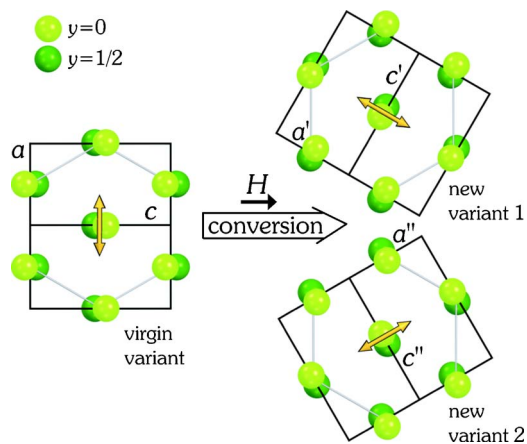


FIG. 2. (Color online) The rare earth atomic positions before (left) and after (right) the conversion with the magnetic field perpendicular to the easy axis [ $\angle(H, a) = 90^\circ$ ]. Effectively the unit cell is rotated. The virgin TV gets entirely depopulated. Two new twin variants arise. Only the rare earth ions are shown. The double arrows symbolize the easy axis. The hexagon shows the idealized austenite state.

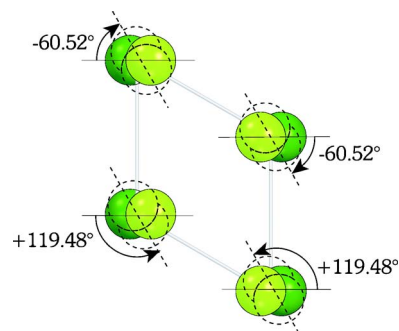


FIG. 3. (Color online) Atomic movement during the shift of the twin boundary shown at exemplary rare earth atoms of *new variant 2* from Fig. 2. The converted state is symbolized by the dotted shape. One may interpret the diffusionless atomic shift as a rotation about the  $b$  axis.

$= 1.56^\circ$ ) occurs. In our case, with the field parallel to the hard axis, the occurrence of three twin variants at the same time could not be avoided. But, we expect to be able to prevent intrinsic strain by applying the magnetic field in a way that only two twin variants will occur at a time, e.g., the field along the easy axis of one of the new twin variants.

### III. NEUTRON SCATTERING EXPERIMENT

To prove the model a neutron scattering experiment has been performed at the Hahn-Meitner-Institut Berlin at the E2 instrument which provides a flat-cone option. We have chosen a  $Tb_{0.5}Dy_{0.5}Cu_2$  single crystal because it has the lowest known conversion field. It has been grown by Thomas Reif with the Czochralski method in the Forschungszentrum Jülich. Its quality greatly fulfilled the demand of the experiment. The dimension of the cuboid shaped sample was  $4 \times 4 \times 3 \text{ mm}^3$ . The sample was clamped from four sides by an aluminium frame. The magnetic field was applied parallel to the  $c$  direction which is the magnetic hard direction of the virgin variant. We have chosen a conversion temperature of 29 K in this experiment. This temperature has been found out to be the temperature with minimal conversion field (see Sec. IV).

The movement of a twin boundary—or in other words the conversion between twin variants—leads crystallographically to a rotation of the crystal structure about the  $b$  axis by  $60.52^\circ$  corresponding to a translation of each rare earth atom by either  $0.29(1) \text{ \AA}$  or  $0.50(1) \text{ \AA}$  within the pseudohexagonal  $ac$  plane (Fig. 2). When considering two planes, this is identical to a rotation of atomic pairs around an axis parallel to  $b$  as shown in Fig. 3.

In neutron scattering one expects nuclear reflections corresponding to the virgin variant to drastically lose intensity. On the other hand, emerging twin variants will be indicated by occurring reflections which are partially at completely new positions.

To identify reflections from the three twin variants unequivocally, we use orthorhombic notation and include indices to the reflection syntax numbering the twin variants from zero to two, e.g.  $(2\ 0\ 0)_0$  is a reflection of the virgin variant,

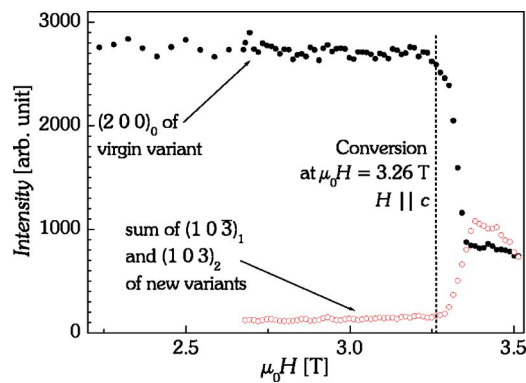


FIG. 4. (Color online) Field dependent intensities of the  $(2\ 0\ 0)_0$  reflection (full spheres) and of the emerging  $(1\ 0\ \bar{3})_1$  and  $(1\ 0\ 3)_2$  reflections (empty spheres). Intensities were integrated within the two-theta regions with a fixed sample rotation at  $T=29$  K. Since the reflections are only  $0.4^\circ$  apart in two-theta the integration regions of both curves overlap slightly. The background has not been subtracted.

$(1\ 0\ \bar{3})_1$  and  $(1\ 0\ 3)_2$  are reflections from the two other variants.

Because the crystal does not have an exact hexagonal structure, reflections of converted TVs are not at exact integer and half-integer  $(h\ k\ l)_0$  positions with respect to the initial sample orientation. For instance reflections at the  $(h\ k\ \frac{1}{2})_0$  plane are located at  $l = \frac{1}{2} \pm 0.0091 \cdot h$ . However, since the vertical detector collimation is relaxed by  $3^\circ$  all reflections could be covered.

Within the resolution of the experiment, often reflections from different TVs, appearing at an almost identical position in  $q$  space, could not be distinguished. Therefore, the integrated intensity over a small region at the according  $q$  vector, covering reflections from multiple TVs, had *always* been considered for evaluation.

At a magnetic field of 3.26 T and 29 K, for instance, the  $(2\ 0\ 0)_0$  reflection starts to vanish, whereas at a very similar position, the  $(1\ 0\ \bar{3})_1$  and  $(1\ 0\ 3)_2$  reflection coinstantaneously emerges. As a certain exemption, the  $(2\ 0\ 0)_0$  reflection *could* be distinguished from the sum of the converted  $(1\ 0\ \bar{3})_1$  and  $(1\ 0\ 3)_2$  reflection. The difference in their scat-

tering angle is  $\Delta_{2\theta} = 0.4^\circ$  and therefore just above the instrument resolution which is  $0.2^\circ$ . The integrated intensities are shown in Fig. 4.

Due to the crystallographic rotation, for  $k$  being odd, reflections at half-integer  $h$  and  $l$  values occur in  $(h\ k\ l)_0$ . For example the  $(0\ 3\ 1)_0$  reflection rotates about the  $k$  axis to the scattering position  $(\frac{1}{2}\ 3\ \frac{1}{2})_0 \triangleq (0\ 3\ 1)_2$ . Therefore we measured, additionally to the  $(h\ k\ 0)_0$  and  $(h\ k\ 1)_0$  planes, also the  $(h\ k\ \frac{1}{2})_0$  plane at  $T_{\text{conv}} = 29$  K and at  $T = 54\ \text{K} > T_N$  before and after the conversion.

Figure 5 compares the  $(h\ k\ \frac{1}{2})_0$  scattering planes before and after the twin-variant conversion. The appearance of new reflections in the  $(h\ k\ \frac{1}{2})_0$  scattering plane at expected scattering positions and with expected intensities supports the TV model. The converted state has been found to remain when the magnetic field is removed and/or the crystal is heated into the paramagnetic state ( $T_N = 38\ \text{K}$ ) or even to room temperature.<sup>17</sup> Thus one can confirm that the conversion is associated with a microstructural change and is not a phase change. This observation is contradictory to the perception of a metamagnetic state delineated in Ref. 9.

To analyze the structural changes we evaluated the nuclear intensities in the paramagnetic state at zero field. As mentioned above reflections from different twin variants often are at indistinguishable scattering positions. For the analysis the according region had been integrated. The composition of respective  $q$  regions and according intensities before and after the twin-variant conversion are shown in Table I. As expected for a virgin crystal no intensity was found in the  $(h\ k\ \frac{1}{2})_0$  plane reflected by the fourth column. Nuclear scattering intensities at 54 K taken before the conversion agree with the known crystallographic structure.<sup>18</sup> Therefore no refinement of structure parameters was necessary for our question. Theoretical intensities after the conversion were calculated by summarizing the three twin variants assuming for each variant the identical virgin crystal structure and fitting for each variant a scaling factor. The comparison of measured intensities after the conversion with theoretical intensities provides a good agreement to the twin-variant model. The crystal structure of converted twin variants is thus identical to the virgin structure.

The decrease of intensity of  $(0\ 3\ 1)_0$ ,  $(2\ 3\ 1)_0$ ,  $(0\ 5\ 1)_0$ , and  $(2\ 7\ 1)_0$  suggests a decrease of the volume fraction of

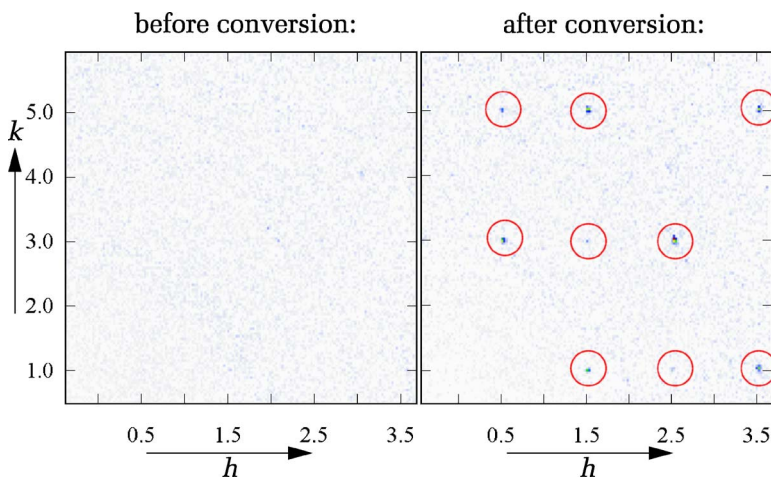


FIG. 5. (Color online)  $(h\ k\ \frac{1}{2})_0$  planes measured with neutron scattering on  $\text{Tb}_{0.5}\text{Dy}_{0.5}\text{Cu}_2$  at  $T=30$  K before and after the application of the field. Reflections on the right picture appear due to emerging twin variants.

TABLE I. Normalized intensities measured at 54 K and 0 T, before and after the conversion,  $H\parallel c$ . Intensities after conversion are composed of reflections of one, two, or three TVs.

Virgin ( $h k l$ ) <sub>0</sub>	New 1 ( $h k l$ ) <sub>1</sub>	New 2 ( $h k l$ ) <sub>2</sub>	Before Conversion		After Conversion	
			Calc.	Expt.	Calc.	Expt.
(2 0 0) <sub>0</sub>	(1 0 $\bar{3}$ ) <sub>1</sub>	(1 0 3) <sub>2</sub>	1001	1001	1366	1100
(2 2 0) <sub>0</sub>	(1 2 $\bar{3}$ ) <sub>1</sub>	(1 2 3) <sub>2</sub>	0	0	21	26
(0 4 0) <sub>0</sub>	(0 4 0) <sub>1</sub>	(0 4 0) <sub>2</sub>	282	293	488	420
(2 4 0) <sub>0</sub>	(1 4 $\bar{3}$ ) <sub>1</sub>	(1 4 3) <sub>2</sub>	219	233	258	243
(0 6 0) <sub>0</sub>	(0 6 0) <sub>1</sub>	(0 6 0) <sub>2</sub>	209	531	358	520
(4 0 0) <sub>0</sub>	(2 0 $\bar{6}$ ) <sub>1</sub>	(2 0 6) <sub>2</sub>	490	362	354	165
(4 2 0) <sub>0</sub>	(2 2 $\bar{6}$ ) <sub>1</sub>	(2 2 6) <sub>2</sub>	0	0	124	93
(2 6 0) <sub>0</sub>	(1 6 $\bar{3}$ ) <sub>1</sub>	(1 6 3) <sub>2</sub>	184	207	219	238
(4 4 0) <sub>0</sub>	(2 4 $\bar{6}$ ) <sub>1</sub>	(2 4 6) <sub>2</sub>	147	121	53	15
( $\frac{1}{2}$ 3 $\frac{1}{2}$ ) <sub>0</sub>	...	(0 3 1) <sub>2</sub>	0	0	196	188
( $\frac{3}{2}$ 3 $\frac{1}{2}$ ) <sub>0</sub>	(1 3 $\bar{2}$ ) <sub>1</sub>	...	0	0	21	19
( $\frac{5}{2}$ 1 $\frac{1}{2}$ ) <sub>0</sub>	...	(1 1 4) <sub>2</sub>	0	0	27	23
( $\frac{5}{2}$ 3 $\frac{1}{2}$ ) <sub>0</sub>	...	(1 3 4) <sub>2</sub>	0	0	279	280
( $\frac{1}{2}$ 5 $\frac{1}{2}$ ) <sub>0</sub>	...	(0 5 1) <sub>2</sub>	0	0	66	45
( $\frac{3}{2}$ 5 $\frac{1}{2}$ ) <sub>0</sub>	(1 5 $\bar{2}$ ) <sub>1</sub>	...	0	0	206	205
( $\frac{7}{2}$ 1 $\frac{1}{2}$ ) <sub>0</sub>	(2 1 $\bar{5}$ ) <sub>1</sub>	...	0	0	134	123
( $\frac{1}{2}$ 7 $\frac{1}{2}$ ) <sub>0</sub>	...	(0 7 1) <sub>2</sub>	0	0	79	75
( $\frac{3}{2}$ 7 $\frac{1}{2}$ ) <sub>0</sub>	(1 7 $\bar{2}$ ) <sub>1</sub>	...	0	0	9	12
( $\frac{7}{2}$ 5 $\frac{1}{2}$ ) <sub>0</sub>	(2 5 $\bar{5}$ ) <sub>1</sub>	...	0	0	252	290
(1 0 1) <sub>0</sub>	(1 0 $\bar{1}$ ) <sub>1</sub>	(0 0 2) <sub>2</sub>	53	59	51	50
(1 2 1) <sub>0</sub>	(1 2 $\bar{1}$ ) <sub>2</sub>	(0 2 2) <sub>2</sub>	348	425	805	1070
(0 3 1) <sub>0</sub>	...	...	365	365	54	77
(1 4 1) <sub>0</sub>	(1 4 $\bar{1}$ ) <sub>1</sub>	(0 4 2) <sub>2</sub>	122	111	133	133
(2 3 1) <sub>0</sub>	...	...	255	243	37	36
(3 0 1) <sub>0</sub>	...	(1 0 5) <sub>2</sub>	20	12	13	10
(0 5 1) <sub>0</sub>	...	...	122	125	18	13
(3 2 1) <sub>0</sub>	(2 2 $\bar{4}$ ) <sub>1</sub>	(1 2 5) <sub>2</sub>	355	313	205	128
(3 4 1) <sub>0</sub>	(2 4 $\bar{4}$ ) <sub>1</sub>	...	84	84	21	13
(2 7 1) <sub>0</sub>	...	...	133	122	20	21

the virgin TV down to 16(1)% sufficiently close to the expected complete depopulation. The new variants volume fraction had been determined to be 40(5)% and 44(5)%. The approximate equal distribution fits to the expectation of the model where for  $H\parallel c$  (=hard axis) both new variants are expected to have the same probability.

#### IV. MAGNETIZATION AND STRAIN

In the following the consequences of the conversion on macroscopic magnetization and magnetostrain is examined. Figure 6 shows the magnetization during the conversion. In a magnetic field below the conversion field  $H_c$ , which had been applied parallel to the (hard)  $c$  direction, the magnetic moments are rotated continuously from the magnetic easy  $a$

axis to the direction of the field. At  $H_c$ , however, the magnetization increases suddenly (Fig. 6), due to the formation of two new twin variants (Fig. 2, right). The vectorial superposition of both of their magnetization curves are now similar compared to the magnetization curve of the initial magnetic easy  $a$  axis (not shown in the figure).<sup>17</sup> Because of this, in former publications an exchange of magnetic axes without a microstructural change had been concluded.<sup>2-8</sup>

Ramping down the field and repeating the magnetic field scan afterwards the magnetization jump does not occur anymore. The magnetic behavior now is similar to the easy  $a$  axis. This is a typical behavior of MSM compounds: Once the easy axes are aligned in a low energy configuration towards the external field, no large hysteresis occurs.<sup>19</sup> In contrast to conventional MSM, the conversion process takes



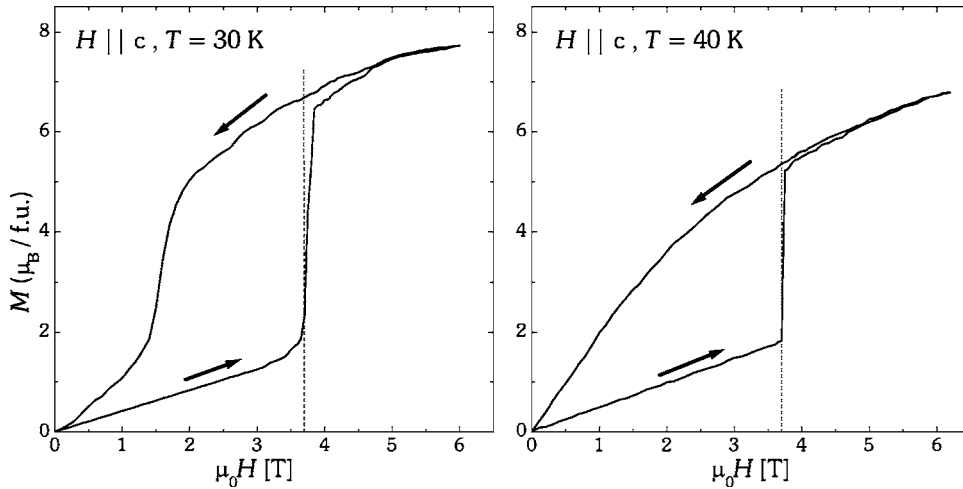


FIG. 6. Magnetization on  $\text{Tb}_{0.5}\text{Dy}_{0.5}\text{Cu}_2$  below and above the Néel temperature  $T_N=38$  K showing a jump in magnetization and thus a significant change in the magnetic easy axis.

place not only below the magnetic ordering temperature  $T_N=38$  K, but also in the paramagnetic region. The magnetization curve at  $T=40$  K, presented on the right part of Fig. 6, shows a conversion field of  $H_c=3.7$  T. As one can see by the differences of the virgin and converted state, the AF state as well as the paramagnetic state have a strong anisotropy. The higher moment in the converted state shows that the easy axis is now preferentially aligned along the external field.

The magnetization measurements were repeated at different temperatures to investigate the temperature dependence of the conversion field. The summarized result is shown in Fig. 7. The field which is necessary to create new twin variants in a virgin single-variant sample has a minimum of about 3.6 T at 30 K. It decreases for further conversions on the same sample (not shown in the figure), what is called “training of the sample.”

The AF order with no net magnetization requires a higher field to induce a sufficient magnetization to reach a free energy difference of both variants in order to start the conversion process. Therefore the conversion field increases to lower temperatures. On the other hand the increase of the

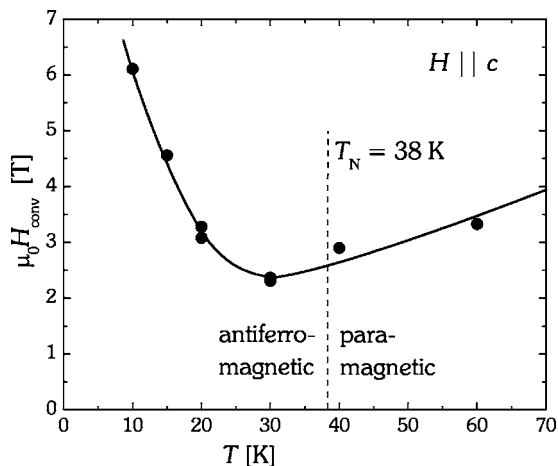


FIG. 7. Variant-conversion field depending on the temperature measured on trained  $\text{Tb}_{0.5}\text{Dy}_{0.5}\text{Cu}_2$  samples (see text). Even above the Néel temperature a variant conversion is possible.

conversion field to higher temperatures shows the influence of the lower magnetic anisotropy due to thermally fluctuating moments.

To study the influence of the twin-variant conversion on the macroscopic sample size we measured the strain of  $\text{Tb}_{0.5}\text{Dy}_{0.5}\text{Cu}_2$  using a capacitive miniature dilatometer.<sup>20</sup> From Fig. 2 an estimate for the length change can be derived,  $\Delta c/c=2 \cdot (1+(c^2/a^2))^{-(1/2)}-1$  and  $\Delta a/a=\frac{1}{2} \cdot (1+(c^2/a^2))^{1/2}-1$ . The measurements, performed at  $T=30$  K in fields along the  $c$  axis, yield an expansion of the sample length in  $c$  direction of about  $\Delta c/c=1.5(3)\%$  which is in agreement with the theoretical magnetostriction of 1.59%. Similar data had been already measured for  $\text{DyCu}_2$  and  $\text{TbCu}_2$ .<sup>21</sup> In the case of  $\text{TbCu}_2$  the measurements could not be completed because of the formation of microcracks at the conversion process.

## V. DISCUSSION

During the conversion the atoms change their spatial position without atomic diffusion (Fig. 3). Since the crystal structure of  $RCu_2$  is nearly hexagonal, the new position of the atoms is close by. The atomic movement is driven by the coupling of the rare earths local-moment direction to the anisotropy of the  $4f$ -charge density. Rare earth ions and especially Tb have a strongly aspherical  $4f$ -charge density connected to a localized spin moment. If a magnetic field is applied, the  $4f$  moment changes and consequently also the  $4f$  charge density changes. The rotation of a rare earth ion at a twin boundary, feeling the crystal fields of both variants, results in a rejection to the virgin variant and an attraction towards the new variant. As long as the transition has not happened, which is below the conversion field, the process is reversible. A removal of the field would lead to the initial state.

Without an external magnetic field all three potential minima of the elastic energy, more precisely the potential of the virgin variant and the two yet vacant potentials of the new variants have the same magnitude separated by a potential barrier. With application of the external conversion field

one increases the ions magnetocrystalline anisotropy energy (McAE) in the whole crystal. An additional energy gain due to crystal imperfections can be assumed at certain locations. There the growth of new twin variants will occur. The energy gain from the twin boundary together with the influence of the external field leads to a snowball-like growth of new twin variants as observed in the experiment.

## VI. SUMMARY

In  $RCu_2$  a magnetically-induced conversion effect is known for 15 years but had not been understood yet. With usage of the neutron-scattering investigation method it actually was possible to observe the structural changes during the conversion in  $Tb_{0.5}Dy_{0.5}Cu_2$ . A new model is presented explaining macroscopic observations on  $RCu_2$  compounds, found in the past: the *twin-variant model*. The basic idea of the model is a diffusion-free microstructural change in which the volume fraction for three twin variants with identical crystal structure changes.

In fact, experimental results presented in this paper give evidence for MSM behavior at  $Tb_{0.5}Dy_{0.5}Cu_2$ . Since the crystallographic structure of  $Tb_{0.5}Dy_{0.5}Cu_2$  is qualitative identical to other  $RCu_2$  compounds, we assume the observed mechanism is applicable for all  $RCu_2$  compounds.

The presented new MSM-compound system  $RCu_2$  has remarkable qualities distinguishing itself from conventional MSM compounds. The movement of twin boundaries and therefore the conversion effect is possible without magnetic ordering. Thus, it has been shown, that merely the magnetic anisotropy itself is necessary for the MSM effect, where the certain origin for the anisotropy is of no importance. Concerning  $RCu_2$ , the magnetic anisotropy originates from the crystal field mediated by the  $4f$ -charge distribution where an anisotropy due to magnetic exchange interaction is not necessary.

$RCu_2$  is, besides  $La_{2-x}Sr_xCuO_4$ , the second known antiferromagnetic MSM-compound system.<sup>16</sup>

The  $RCu_2$  compound system has an orthorhombic crystal structure close to the hexagonal structure. This structure can be understood to be a martensitic state where three twin variants can easily occur. To our knowledge, the associated high-symmetric hexagonal austenitic state does not exist leading to another difference to conventional MSM compounds, where magnetic order usually occurs above the martensitic transition.

One can summarize the following two criteria for the occurrence of the MSM effect: (1) The crystallographic structure has to be *close enough* to a higher symmetric but not necessarily appearing structure to potentiate twin variants. (2) A magnetic anisotropy is necessary, which is sufficiently strong coupled to the structure to overcome the potential barrier. It has been shown, that the magnetic anisotropy is separated from the demand of magnetic exchange or ordering exchange.

The paramagnetic MSM effect in intermetallic compounds containing rare earth elements with their strong magnetocrystalline anisotropy opens a new and promising field of science and increases the possibilities for further applications.

## ACKNOWLEDGMENTS

We would like to thank Sebastian Fähler from the IFW Dresden for his contribution to our work. We further thank Sirko Kramp for his inciting suggestions during his Ph.D. research. We thank Ulrike Witte and Chen Xing-Qiu for their experimental support. We would like to thank Thomas Reif for the  $Tb_{0.5}Dy_{0.5}Cu_2$  sample preparation. We gratefully acknowledge the financial support by the Deutsche Forschungsgemeinschaft from the SFB 463 as well as from the Hahn-Meitner-Institut Berlin. We acknowledge the support by the Austrian Science Foundation (FWF) P17226, P16250.

\*Also at HMI Berlin; Electronic address: raasch@hmi.de

- <sup>1</sup>Y. Hashimoto, A. Yamagishi, T. Takeuchi, and M. Date, *J. Magn. Magn. Mater.* **90–91**, 49 (1990).
- <sup>2</sup>K. Sugiyama, P. Ahmet, M. Abliz, H. Azuma, T. Takeuchi, K. Kindo, H. Sugawara, K. Motoki, R. Settai, and Y. Onuki, *Physica B* **211**, 145 (1995).
- <sup>3</sup>R. Settai, M. Abliz, P. Ahmet, K. Motoki, N. Kimura, H. Ikezawa, T. Ebihara, H. Sugawara, K. Sugiyama, and Y. Onuki, *J. Phys. Soc. Jpn.* **64**, 383 (1995).
- <sup>4</sup>K. Sugiyama, Y. Yoshida, A. Koyanagi, R. Settai, T. Takeuchi, K. Kindo, and Y. Onuki, *J. Magn. Magn. Mater.* **177–181**, 361 (1998).
- <sup>5</sup>K. Sugiyama, M. Nakashima, Y. Yoshida, Y. Kimura, K. Kindo, T. Takeuchi, R. Settai, and Y. Onuki, *J. Phys. Soc. Jpn.* **67**, 3244 (1998).
- <sup>6</sup>S. Kramp, M. Doerr, M. Rotter, M. Loewenhaupt, and R. van de Kamp, *Eur. Phys. J. B* **18**, 559 (2000).
- <sup>7</sup>K. Sugiyama, T. Yamamoto, N. Nakamura, K. Kindo, R. Settai, and Y. Onuki, *J. Magn. Magn. Mater.* **262**, 389 (2003).

- <sup>8</sup>Y. Hashimoto, K. Kindo, T. Takeuchi, K. Senda, M. Date, and A. Yamagishi, *Phys. Rev. Lett.* **72**, 1922 (1994).
- <sup>9</sup>Y. Yoshida, K. Sugiyama, T. Takeuchi, Y. Kimura, D. Aoki, M. Kouzaki, R. Settai, K. Kindo, and Y. Onuki, *J. Phys. Soc. Jpn.* **67**, 1421 (1998).
- <sup>10</sup>T. Takeuchi, P. Ahmet, M. Abliz, R. Settai, and Y. Onuki, *J. Phys. Soc. Jpn.* **65**, 1404 (1996).
- <sup>11</sup>P. Svoboda, M. Doerr, M. Loewenhaupt, M. Rotter, T. Reif, F. Bourdarot, and P. Burlet, *Europhys. Lett.* **48**, 410 (1999).
- <sup>12</sup>K. Ullakko, J. K. Huang, C. Kantner, R. C. O’Handley, and V. V. Kokorin, *Appl. Phys. Lett.* **69**, 1966 (1996).
- <sup>13</sup>S. J. Murray, M. Marioni, S. M. Allen, R. C. O’Handley, and T. A. Lograsso, *Appl. Phys. Lett.* **77**(6), 886 (2000).
- <sup>14</sup>R. D. James and M. Wulping, *Philos. Mag. A* **77**(5), 1273 (1998).
- <sup>15</sup>J. Enkovaara, A. Ayuela, A. T. Zayak, P. Entel, L. Nordstroem, M. Dube, J. Jalkanen, J. Impola, and R. M. Nieminen, *Mater. Sci. Eng., A* **378**, 52 (2003).
- <sup>16</sup>A. N. Lavrov, S. Komiya, and Y. Ando, *Nature (London)* **418**, 385 (2002).

- <sup>17</sup>M. Loewenhaupt, M. Doerr, M. Rotter, T. Reif, and A. Schneidewind, *Braz. J. Phys.* **30**, 754 (2000).
- <sup>18</sup>A. R. Storm and K. E. Benson, *Acta Crystallogr.* **16**, 701 (1963).
- <sup>19</sup>O. Heczko, L. Straka, N. Lanska, K. Ullakko, and J. Enkovaara, *J. Appl. Phys.* **91**, 8228 (2002).
- <sup>20</sup>M. Rotter, E. Gratz, H. Mueller, M. Doerr, and M. Loewenhaupt, *Rev. Sci. Instrum.* **69**, 2742 (1998).
- <sup>21</sup>M. Doerr, M. Rotter, M. Loewenhaupt, T. Reif, and P. Svoboda, *Physica B* **284–288**, 1331 (2000).